DINAME 2023 - Proceedings of the XIX International Symposium on Dynamic Problems of Mechanics,
A.S. De Paula, A.T. Fabro and M.R. Machado (Editors), ABCM.
Pirenópolis, Go, Brazil, February 26th to March 3rd, 2023

# A comparison of two drill-string models that include the dynamics of the cutting at the bit

**H. E. Goicoechea[1,2], R. Lima[1] , F. Buezas[2] and R. Sampaio[1]**

[1] Pontifícia Universidade Católica do Rio de Janeiro, Mechanical Engineering Department, Avenida Marquês de São Vicente 255, Gávea, 22451-900, Rio de Janeiro, RJ, Brazil

[2] Instituto de Física del Sur (IFISUR), Departamento de Física, Universidad Nacional del Sur, CONICET, Av. L. N. Alem 1253, Bahía Blanca, B8000CPB, Buenos Aires, Argentina

*Abstract: In this paper, a comparison of the two dynamics predicted by two different models of a drill-string is made. All the simulations consider a structure that is* 1200 *m long, with the same geometric and material set of parameters. In the first model, an established two degrees-of-freedom (DOF) formulation is used, with 1-DOF for the axial dynamics and 1-DOF for the torsional one. The second model uses the same 1-DOF axial formulation and a wave-equation for the torsional shaft. In both cases, the structural dynamics are coupled with the dynamics of the cutting through the depth-of-cut used in the bit-rock interaction relation. In both models an advection equation is solved along with the equations of motion to calculate the previous depth. The major contributions of the study are: 1) the modelling of the cutting by means of a bit-rock interaction relation, that among other parameters, depends on an instantaneous depth-of-cut, and that does not restrict backward rotation nor bit-bounce; 2) the calculation of the depth-of-cut through the resolution of an advection equation, as an alternative to introducing delays in the system of differential equations; 3) the extension of the advection approach to allow rotation in both directions; 4) the combination of the previous items with a distributed representation to account for the torsional dynamics; 5) the inclusion of the 2-DOF model as a limiting case of the continuous model, for which a strategy introducing an extra parameter* $\alpha$ *is used. Some application cases considering different operation conditions are simulated. The results show that the dynamics can differ considerably. This suggests that the second model, with a continuous torsional shaft, could be capturing aspects of the dynamics that are neglected in the first model, with the 2-DOF approach. On top of that, some comments regarding the choice of one approach over the other are made.*

***Keywords: Drill-string dynamics, soil cutting, advection equation in cutting, torsional oscillations, stick-slip***

## INTRODUCTION

Drill-strings are very slender structures used in the extraction of oil and gas. They are composed of tubes that are responsible for transmitting the forces and torques from the top of a well to the bit, at the other end. These structures may undergo complex dynamics, exhibiting vibrations and stick-slip, as in Lima and Sampaio (2015); Saldivar *et al.* (2016), as well as buckling and other phenomena.

With regard to the modelling of drill-strings, both discrete and continuous models are found in the literature. On the one hand, among the papers that aim at capturing the dynamics of a real-scale structure using lumped formulations, Richard *et al.* (2007) present a 2 degrees-of-freedom (DOF) model to study the cause of drill-string stick-slip vibrations. The authors study a theoretical blunt polycrystalline diamond compact (PDC) cutter, and they use a velocity-dependent bit-rock interaction law in a model that also accounts for the dynamics of the cutting. The predictions show that self-excited vibrations can appear in this model. Self-excited vibrations had also been the object of similar studies, although a velocity-dependent interaction law had been used instead. The velocity-dependent approach is frequently found in previous work before Richard *et al.* (2007). For this reason, the model of Richard *et al.* (2007) introduced the novelty that self-excited vibrations can arise even if an interaction law that is not velocity dependent is used, what suggests that the velocity weakening interface law generally assumed to be an intrinsic property of the bit rock interaction is actually a consequence rather than a cause of the self-excited vibrations.

On the other hand, continuous models are used in Trindade and Sampaio (2005); Sampaio *et al.* (2007); Piovan and Sampaio (2009); Goicoechea *et al.* (2019); Aarsnes and van de Wouw (2019), to name some. In those works different continuous bar-shaft representations are used. In particular, Aarsnes and van de Wouw (2019) employs a distributed axial-torsional approach, and it shows "how multiple axial modes are excited or attenuated, depending on the bit rotation rate", and therefore it is suggested that "a lumped drill-string approximation is insufficient for the general case", with regard to the behaviour observed in the axial dynamics.

Given the different formulations found across studies concerning drill-string dynamics, there is no clear consensus towards the choice of an optimal model for drill-strings. This choice might be motivated by the integration run-time, simplicity, or the capacity to tackle the problem analytically, which is often more difficult when continuous formulations are employed. The objective of this work is to show that to use a 1- or 2-DOF model to simulate the dynamics of a real

scale drill-string may result in an oversimplification of the problem, and it could lead to inaccurate results. This study represents a first step to assess the suitability of the different approaches, where the bit-rock interaction forces are the only responsible for the dissipative terms considered. The analysis presented in this article is an excerpt of the work carried out in Goicoechea *et al.* (2022).

## THE DRILL-STRING MODELS

In this study, the predictions obtained by two different models, namely M1 and M2, are compared. A sketch showing the details of each model is provided in Fig. 1.

Model M1 is a modified version of the 2-DOF (1-torsional, 1-axial) formulation used in Richard *et al.* (2007). The original model in Richard *et al.* (2007) calculates the depth-of-cut by evaluating the position in the current time, as well as in previous instants. Thus, it introduces a set of delays in the system of differential equations. The modified version of the model takes an extended version of the bit-rock interaction relations, avoiding the introduction of delays by solving an extra advection equation to calculate the instantaneous depth-of-cut.

The model M2 is similar to that used in M1, although the torsional dynamics are tackled with a continuous formulation, while retaining a 1-DOF approach for the axial motion.

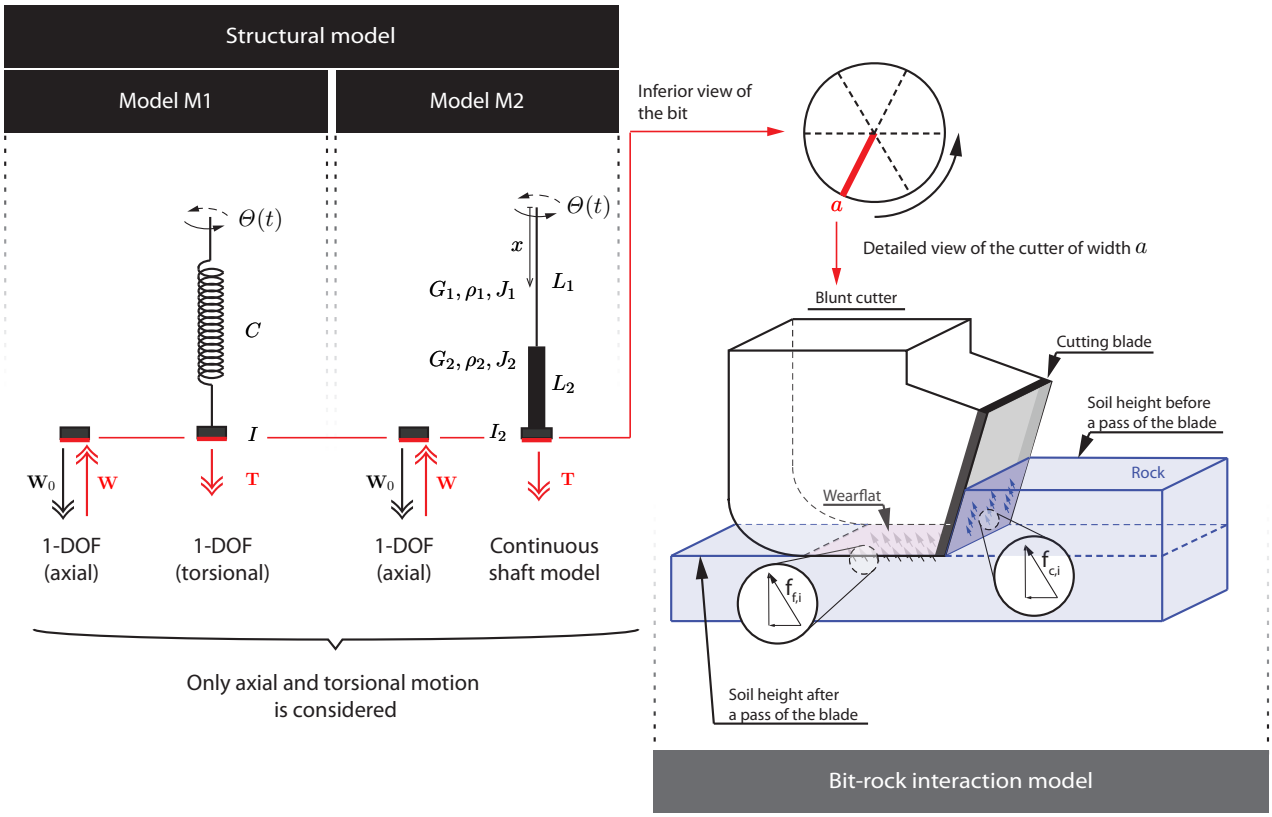


Figure 1: A sketch showing the two models employed, M1 and M2. Model M1: $M$ is a mass, $I$ an inertia, $C$ a spring constant. Model M2: two different cross-sections are considered with $J_1$, $J_2$ being the geometric moment of inertia of the drill-pipes and the bottom hole assembly (BHA), respectively; $G_1$, $G_2$ the shear elastic moduli; and $\rho_1$, $\rho_2$ the densities of the material. At the lower end, a concentrated inertia $I_2$ is considered. $\mathbf{W}, \mathbf{W}_0$ and $\mathbf{T}$ are generalised forces.

### The axial dynamics model

The torsional dynamics are given by

$$M\frac{d^2U}{dt^2} = W - W_0 \tag{1}$$

where $U$ is the position of the bit, $W_0$ is the magnitude of the difference between the submerged weight and the hook load and $W$ the magnitude of a reaction force due to the bit-rock interaction.

### Torsional dynamics - Model M1

The torsional dynamics are given by

$$I\frac{d^2\Phi}{dt^2} + C(\Phi - \Theta) = T \tag{2}$$

where $\Phi$ is the angular displacement of the bit, $C$ a spring constant to account for the rigidity of the drill-pipes, $I$ the concentrated inertia to account for the bottom hole assembly (BHA) and $T$ the torque-on-bit due to the bit-rock interaction.

### Torsional dynamics - Model M2

Recalling that in M2 the axial dynamics are also represented by (1), the torsional dynamics are given by

$$G_j J_j \frac{\partial^2 \Phi_j}{\partial x_j^2} = \alpha \rho_j J_j \frac{\partial^2 \Phi_j}{\partial t^2}, \text{with } j = \{1,2\}, \text{ and} \tag{3}$$

where $x_1 \in [0, L_1]$, and $x_2 \in [L_1, L_1 + L_2]$, and a parameter $\alpha \in [0,1]$. Also, the following boundary conditions are used

$$\begin{aligned}
&\Phi_1(x_1 = 0, t) = -\Theta(t), \;\; \Phi_1(x_1 = L_1, t) = \Phi_2(x_2 = L_1, t) \\
&G_1 J_1 \frac{\partial \Phi_1}{\partial x_1}(x_1 = L_1, t) = G_2 J_2 \frac{\partial \Phi_2}{\partial x_2}(x_2 = L_1, t) \\
&G_2 J_2 \frac{\partial \Phi_2}{\partial x_2}(x_2 = L_1 + L_2, t) = T - I_2 \frac{\partial^2 \Phi_2}{\partial t^2}(x_2 = L_1 + L_2, t)
\end{aligned} \tag{4}$$

with $\Phi_j = \Phi_j(x_j, t)$ being the angular displacement of the column, $\Theta(t)$ an imposed rotation at the top, $T$ the torque-on-bit due to the bit-rock interaction.

## THE BIT-ROCK INTERACTION MODEL

An improved version of the bit-rock interaction model presented in Richard *et al.* (2007) is used to define the forces and torques acting at the bit. With the modifications introduced, any assumption limiting backward rotations and bit-bounce is eliminated.

The dynamics of a blunt cutter $i$, like the one depicted in Fig. 2 is considered. The tool has two contact areas, $A_{c,i}$ between the rock and the cutting blade, and $A_{f,i}$ between the wearflat and the rock. The magnitudes of the traction vectors are taken as constants over each contact region (at the cutter and wearflat, respectively). Their value depends on the following characteristic variables:

- The rock contact strength function $\sigma = \sigma(\omega, v)$, defined in terms of two contact strength parameters $\sigma_1$ and $\sigma_2$, and the small regularisation constants $c_1$ and $c_2$;
- The rock intrinsic specific energy function $\varepsilon = \varepsilon(\omega)$, that depends on the intrinsic specific energy parameter $\varepsilon_1$ and a regularisation constant $c_3$;
- the cutter inclination coefficient $\zeta$;
- the coefficient of friction $\mu$;

with $\omega$ and $v$ being the torsional and axial speed of the bit. A sketch of the shape of $\sigma(\omega, v)$ and $\varepsilon(\omega)$ is shown in Fig. 3.

If a symmetric and equiangular distribution of blades is considered, and if all the blades have the same associated parameters bit radius $a_i = a$, depth of cut $d_i = d$, wearflat length $l_i = l$, for $i = \{1, \ldots, n_b\}$, the total force and total torque acting on the bit for the the $n_b$ blades is

$$\mathbf{W} = \mathbf{W}_c + \mathbf{W}_f, \;\; \mathbf{W}_c = \varepsilon(\omega)\zeta a d n_b \mathbf{n}, \;\; \mathbf{W}_f = \sigma(\omega, v) a l n_b \mathbf{n} \tag{5}$$

$$\mathbf{T} = \mathbf{T}_c + \mathbf{T}_f, \;\; \mathbf{T}_c = \frac{1}{2}\frac{a}{\zeta}\mathbf{W}_c, \;\; \mathbf{T}_f = \frac{1}{2} a \mu \gamma \mathbf{W}_f \tag{6}$$

recalling that $W$, $W_c$, $W_f$, $T$, $T_c$, $T_f$ are the magnitudes of the previous vectors.

Finally, the previous expressions (5) and (6) require the calculation of the depth-of-cut, $d$. This is tackled by solving an extra PDE to account for the cutting process, an advection equation.

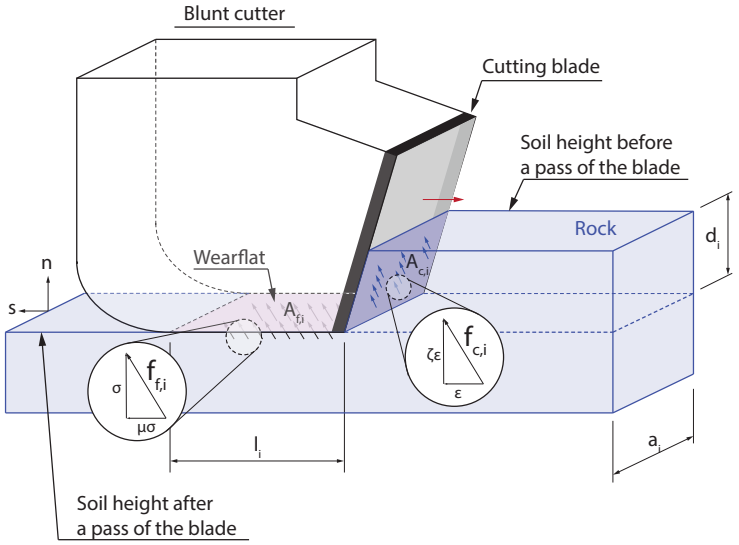


Figure 2: A sketch showing the geometry of the single cutter $i$ is shown. The traction vectors $\mathbf{f}_{f,i}$ and $\mathbf{f}_{c,i}$, acting on the wearflat and the cutting blade, respectively, are drawn. These vectors are defined in terms of the function $\sigma(\omega, v)$, that defines the contact pressure at the wearflat, and $\varepsilon(\omega)$, an intrinsic specific energy of the rock. The parameter $\zeta$ defines the inclination of the cutting force, $\mu$ is the coefficient of friction, $l_i$ is the wearflat length, and $d_i$ is the instantaneous depth of cut.

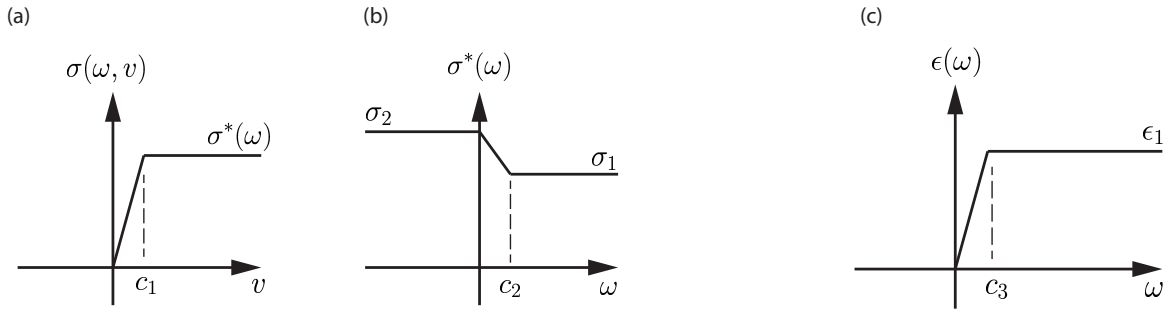


Figure 3: (a) The functional form of $\sigma(\sigma^*(\omega), v)$ is plotted for a fixed value $\omega$; (b) the form of $\sigma^*(\omega)$ is depicted. $\sigma_1$ and $\sigma_2$ are two parameters associated to the rock contact strength. $c_1$ and $c_2$ are some small regularisation constants; and (c) the functional form of $\varepsilon(\omega)$ is shown. $\varepsilon_1$ is a parameter called the rock intrinsic specific energy and $c_3$ is some small regularisation constant.

## Solving the dynamics of the cutting process

The problem of drilling is a free boundary problem, given that the boundary moves as the column advances. Also, the generalised forces change according to the coupled dynamics between the drill-string and the soil interaction at the bit. In particular, the forces depend on the calculation of an instantaneous depth-of-cut. Its magnitude is obtained by solving the an extra advection equation altogether with the previous equations of motion, as proposed by Wahi and Chatterjee (2008). In what follows, the main variable $L_s(\eta, t)$ is used to indicate the position of the soil with respect to some reference (zero). The equation takes the form

$$\frac{\partial L_s}{\partial t} + \omega \frac{\partial L_s}{\partial \eta} = 0, \quad \text{with } \eta \in \left[0, \frac{2\pi}{n_b}\right] \tag{7}$$

where $n_b$ is the number of blades. The advection problem is completed with the boundary conditions below.

$$\text{If } \omega \geq 0,\ L_s(\eta=0,t) = \begin{cases} U(t),\ L_s(\eta=\dfrac{2\pi}{n_b},t) < U(t) \\ \\ L_s(\eta=\dfrac{2\pi}{n_b},t),\ L_s(\eta=\dfrac{2\pi}{n_b},t) \geq U(t) \end{cases} \text{, and if } \omega < 0,\ L_s(\eta=\frac{2\pi}{n_b},t) = L_s(\eta=0,t), \quad (8)$$

which means that cutting can only occur if the bit is rotating in the positive direction. In the previous equations, $U(t)$ is the position of the bit.

Finally, at all times the instantaneous depth of cut is given by

$$d_i = \max\left\{L_s\left(\eta=\frac{2\pi}{n_b},t\right) - L_s\left(\eta=0,t\right),0\right\} \quad (9)$$

## Geometrical interpretation of the equation for the cutting process

A geometrical interpretation for the equation (7) and its boundary conditions, given by (8), is provided in what follows. Figure 4 (a-c) exemplifies the behaviour of (7) for an off-bottom case, i.e. when the bit is rotating without contact with the soil. Meanwhile, Fig. 4 (d-f) shows an example of a normal cutting condition.

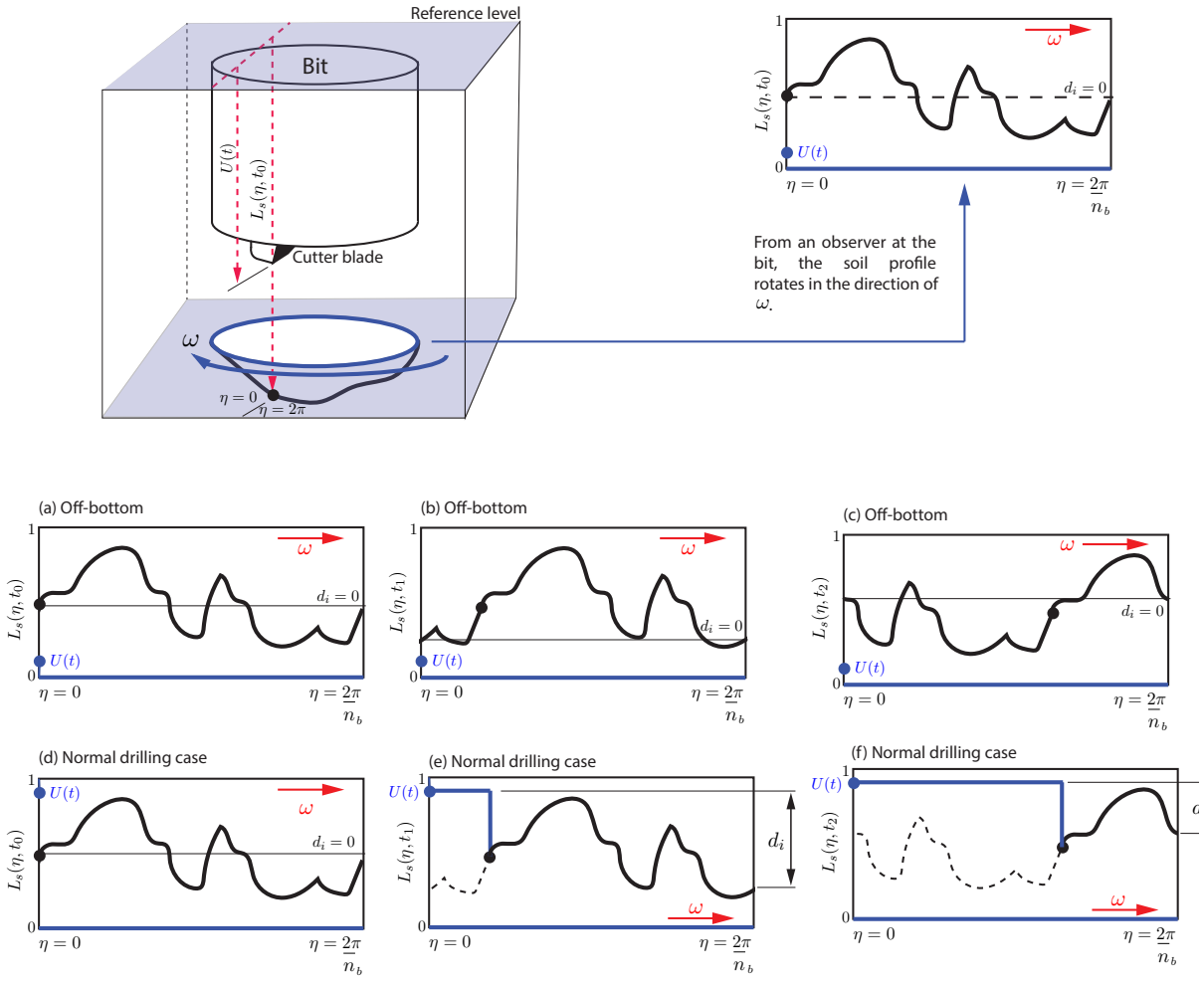


Figure 4: Schematic example of the behaviour of the advection equation to model the cutting process. (a-c) depict an off-bottom case, at times $t_0$, $t_1 > t_0$, and $t_2 > t_1$,, respectively. (d-e) show an example of a normal drilling condition. The red arrow depicts the direction in which the advection equation translate the soil profile with a speed $\omega$.

To begin with, consider a frame that is fixed at the cutting blade, so that the blade is always at angle $\eta = 0$. While drilling, the cutter will move following a circular path over the soil. The equation and the boundary conditions are devised so that the endpoints, $\eta = 0$ and $\eta = \dfrac{2\pi}{n_b}$, represent the soil profile immediately ahead and behind the cutting blade.

In (a), let $L_s(\eta, t = t_0)$ define the soil elevation profile for the off-bottom case. Also, let (b) and (c) be snapshots of the elevation at times $t_1 > t_0$ and $t_2 > t_1$, respectively. In this scenario, the solution of the advection equation in conjunction with periodic boundary conditions give a response that is a translation in space of the solution at time $t_0$. This means, there is no change in the shape of the elevation profile. In addition, the speed at which the soil profile moves spatially is given by $\omega$, thus it is coupled with the torsional equation of motion. Also, it is observed that the endpoints $\eta = 0$ and $\eta = \dfrac{2\pi}{n_b}$ coincide, which means that the instantaneous depth of cut is exactly $d_i = 0$.

Fig. 4 (d-f) show an example of a normal drilling condition. Let (d) be the initial state of the soil profile $L_s(\eta, t = t_0)$. Also, let the position of the bit $U(t = t_0)$ be given by the blue dot, and for this example, let suppose that the position remains constant with time. The fact that $U(t) > L_s(\eta = 0, t)$ indicates that cutting is taking place. Then, (b) and (c) show the evolution of the soil profile at times $t_1 > t_0$ and $t_2 > t_1$. As depicted in the sketch. In contrast with the off-bottom scenario, there is a difference between the values of $L_s(\eta = 0, t)$, the soil height after cutting has taken place, and $L_s(\eta = \dfrac{2\pi}{n_b}, t)$, the soil height before cutting. This difference is the so-called instantaneous depth of cut given by (9). In the figure, the recently removed soil depth is depicted by a dashed line.

## A SPECIAL NON-OSCILLATORY SOLUTION OF THE PREVIOUS EQUATIONS: THE NOMINAL CASE

If a constant angular speed is imposed at the top such that $\Theta(t) = \Omega_0 t$, the formulation employed in models M1 and M2 admits a solution that is non-oscillatory (second time derivatives vanish), for a particular set of initial conditions and boundary conditions, considering a driller operating in the normal cutting regime ($d > 0$, $\omega > 0$, $v > 0$, with $\sigma = \sigma_1$ and $\varepsilon = \varepsilon_1$) This solution will be referred to as "the nominal case".

Some important constant parameters associated to the nominal solution will be calculated: $V_0$ (axial speed), $T_0$ (torque), and $d_0$ (depth of cut), $t_0$ (time taken to complete one turn) and $t_{n0}$ (time taken to cover the separation angle between successive blades).

### The nominal case for model M1

The nominal case for model M1 is characterised by the following parameters

$$\Phi_0 = \Omega_0 t - \frac{T_0}{C}, \;\; V_0 = \Big(W_0 - \sigma_1 a l n_b\Big)\frac{\Omega_0}{2\pi\varepsilon_1 a\zeta} \tag{10}$$

$$d_0 = V_0\, t_{n0} = \frac{V_0 2\pi}{n_b\Omega_0}, \;\; \mathbf{T}_0 = \frac{1}{2}\Big(\varepsilon_1\, d + \mu\gamma\sigma_1\, l\Big)a^2 n_b\mathbf{n} \tag{11}$$

following the derivation procedure in Richard *et al.* (2007).

### The nominal case for model M2

The nominal case for model M2 is characterised by the following parameters

$$\Phi_j(x_j, t) = A_j x_j + B_j(t)\;, \;\; \text{with } j = \{1, 2\}, \tag{12}$$

$$\text{with } A_1 = -\frac{T_0}{GJ_1}, \;\; A_2 = -\frac{T_0}{GJ_2}, \;\; B_1 = \Omega_0\, t, \;\; B_2 = \frac{J_1 L_1 T_0 - J_2 L_2 T_0 + GJ_2 J_1 \Omega_0\, t}{GJ_2 J_1} \tag{13}$$

where $x_1 \in [0, L_1]$, and $x_2 \in [L_1, L_1 + L_2]$,

$$t_0 = \frac{2\pi}{\Omega_0}, \;\; t_{n0} = \frac{2\pi}{n_b\,\Omega_0}, \;\; d_0 = \Big(W_0 - \sigma_1 a l n_b\Big)\frac{1}{\varepsilon_1 a\zeta n_b} \tag{14}$$

$$V_0 = \frac{d_0}{t_{n0}} = \Big(W_0 - \sigma_1 a l n_b\Big)\frac{\Omega_0}{2\pi\varepsilon_1 a\zeta}, \;\; \mathbf{T}_0 = \frac{1}{2}\Big(\varepsilon_1\, d_0 + \mu\gamma\sigma_1\, l\Big)a^2 n_b\mathbf{n} \tag{15}$$

Finally, the nominal solution for the advection equation (so that $d_0$ is a constant) is

$$L_s(\eta, t = 0) = -\frac{d_0\, n_b}{2\pi}\eta \tag{16}$$

| | | Real structure | Model M1 | Model M2 |
|---|---|---|---|---|
| Property | Description | | | |
| $L_1$ | Drill-pipe length | 1000 m | spring (C) | 1000 m |
| $L_2$ | BHA length | 200 m | rigid | 200 m |
| $N_1$ | Number of elements (torsion) | - | – | 64 |
| $N_2$ | Number of elements (advection) | - | 64 | 64 |
| $I, I_2$ | Lumped inertia | - | $I = 112.67$ kgm$^2$ | $I_2 = (1-\alpha)I$ kgm$^2$ |
| $\alpha$ | Artificial parameter | - | - | 1.00 (*) |
| $C$ | Rigidity parameter | - | 469.05 Nm/rad | - |
| $\rho, \rho_1, \rho_2$ | Density | 7800 kg/m$^3$ | | |
| $r_{po}$ | Drill-pipe external radius | 63.5 mm | | |
| $r_{pi}$ | Drill-pipe internal radius | 54.0 mm | | |
| $r_{co}$ | Collar external radius | 76.2 mm | | |
| $r_{ci}$ | Collar internal radius | 28.0 mm | | |
| $G_1, G_2$ | Shear modulus | 77 GPa | | |
| $a$ | Bit radius | 108.0 mm | | |
| $l$ | Drill-bit wearflat length | 1.2 mm | | |
| $\varepsilon_1$ | Rock intrinsic specific energy | 0.252 GPa | | |
| $\sigma_1$ | Rock contact strength | 0.252 GPa | | |
| $\varepsilon_2$ | Rock intrinsic specific energy | 0.504 GPa | | |
| $\sigma_2$ | Rock contact strength | 0.504 GPa | | |
| $M$ | Lumped mass | 24614.40 kg | | |
| $\Omega_0$ | Imposed angular speed | 14.42 rad/s | | |
| $\gamma$ | Drill-bit geometry parameter | 1.00 | | |
| $\zeta$ | Cutter inclination coefficient | 0.38 | | |
| $\mu$ | Coefficient of friction | 0.80 | | |
| $c_1$ | Regularisation constant | $1 \cdot 10^{-5}$ | | |
| $c_2$ | Regularisation constant | $1 \cdot 10^{-1}$ | | |
| $c_3$ | Regularisation constant | $1 \cdot 10^{-3}$ | | |

Table 1: List of parameters employed in the simulation. (*) This parameter varies.

## SIMULATIONS

### Parameters used in the simulations

The parameters employed in this simulation are shown in Tab. 1. The problem is completed with the following initial conditions

$$U(t=0) = 0, \;\; \left.\frac{dU}{dt}\right|_{t=0} = V_0, \;\; L_s(\eta, t=0) = -\frac{d_0\, n_b}{2\pi}\eta \tag{17}$$

with the following conditions for model M1 only

$$\Phi(t=0) = 0, \;\; \left.\frac{d\Phi}{dt}\right|_{t=0} = \Omega_0 + \Delta\Omega_0, \text{with } \Delta\Omega_0 = \Omega_0/10 \tag{18}$$

and the following conditions for model M2 only

$$\Phi_j(x_j, t=0) = 0, \;\; \left.\frac{d\Phi_j}{dt}\right|_{t=0} = \Omega_0 + \frac{\Delta\Omega_0\, x_j}{(L_1+L_2)}, \text{with } \Delta\Omega_0 = \Omega_0/10, \tag{19}$$

where $V_0$ and $\Omega_0$ are constants associated to the nominal solution.

### Simulation 1: Verification considering Model M1 as a limiting case of M2

In what follows, the model M2 is verified by employing a strategy involving controlling the value of the parameter $\alpha$. Model M1 can be interpreted a particular case of M2, if some hypothesis are introduced. The 2-DOF formulation by Richard *et al.* (2007) employs a quasi-static approach, what allows the drill-pipes to be represented by a spring with constant $C$. It also assumes the BHA to be a rigid body. For model M2 to behave like M1, the set of material and geometric parameters need to reflect the previous hypotheses. First, the rigidity of the BHA should be negligible, thus $G_2 \to 0$ needs to be considered. Second, an artificial parameter $\alpha$ is introduced so that the propagation speed of the wave equation, given by $v_w = \sqrt{G/(\alpha\rho)}$, can be controlled. In fact, a quasi-static problem is equivalent to considering an infinite propagation

speed, compatible with taking $\alpha \to 0$. Additionally, the concentrated inertia, $I_2$, in the boundary conditions takes the form $I_2 = (1-\alpha)I$. This expression enables the transition from a fully distributed inertia, for $\alpha = 1.00$, to a fully concentrated inertia when $\alpha \to 0$.

The simulations are calculated using Comsol (COMSOL AB, 2018). The discrete formulation is entered using the ODE equation interface, an the continuous one is introduced in its weak form, in both cases, using Comsol's mathematical module. The advection equation is already programmed in the built-in transport module. It should be noted that only M2 with $\alpha = 1.00$ has a physical meaning. All smaller values just make sense in helping to understand how the response varies from a lumped quasi-static formulation with concentrated inertia to a continuous approach. The angular speed at the bit $\omega(t)$ is plotted in Fig. 5 for (a) $\alpha = 1.00$, (b) $\alpha = 0.80$, (c) $\alpha = 0.40$, (d) model M1.

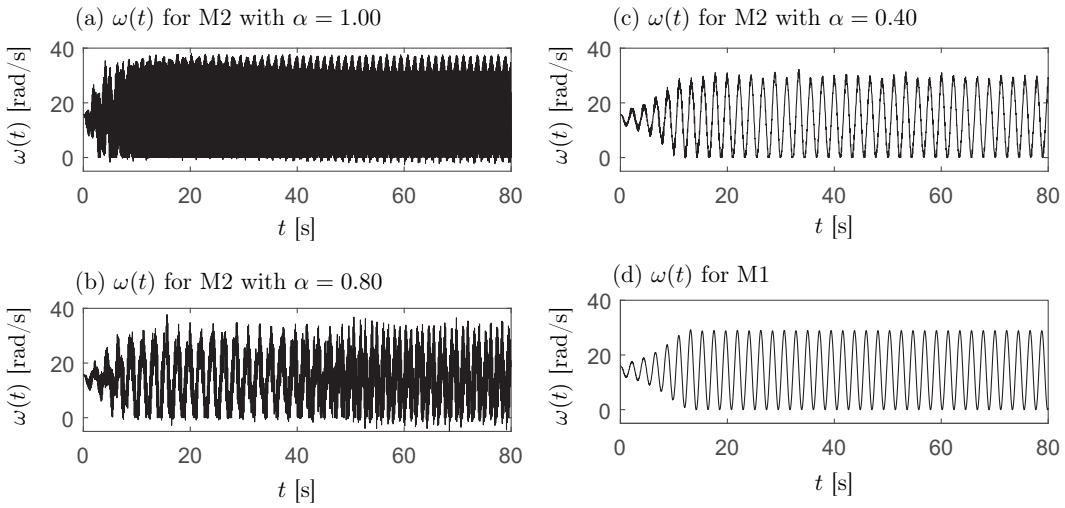


Figure 5: Simulation V2. Angular speed at the bit $\omega(t)$, (a) for model M2 with $\alpha = 1.00$; (b) model M2 with $\alpha = 0.80$; (c) model M2 with $\alpha = 0.40$; (d) Model M1.

It is observed that, as $\alpha$ evolves from 1.00 in Fig. 5(a) to 0.40 in Fig. 5(c), the simulations become more similar to those of Fig. 5(d) calculated with the 2-DOF model.

## Simulation 2: Comparison between the predictions of the two models

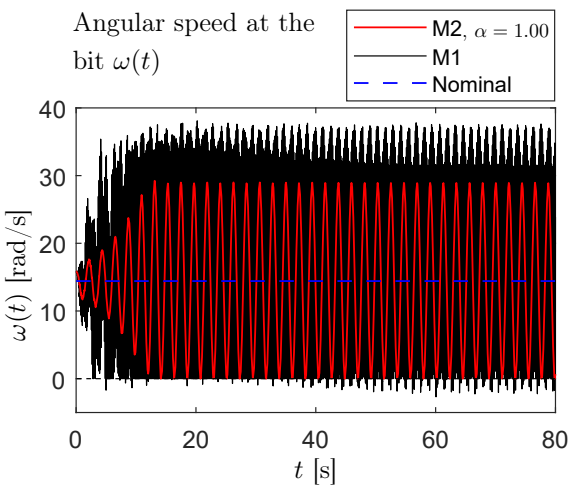


Figure 6: Simulation C1. Angular speed at the bit $\omega(t)$ for the cases C1-A and C1-B (models M1 and M2, respectively). The nominal angular bit speed is shown in dashed line.

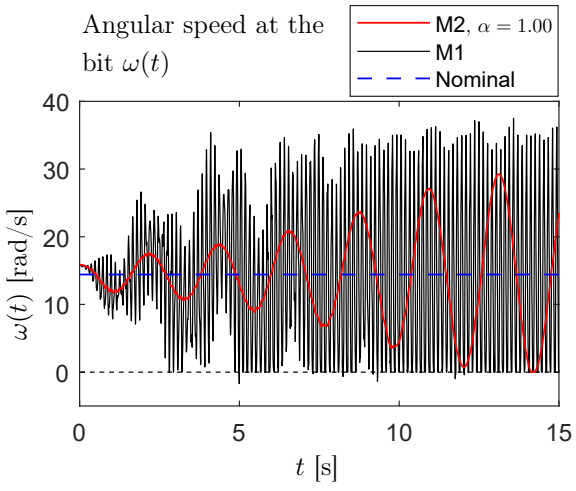


Figure 7: Simulation C1. Angular speed at the bit $\omega(t)$ for the cases C1-A and C1-B (models M1 and M2, respectively). Zoom for $t \in [0\text{s}, 10\text{s}]$. The nominal angular bit speed is shown in dashed line.

A graph overlaying the results for M2 with $\alpha = 1.00$ and M1 is shown in Fig. 6, and a zoomed version is shown in Fig. 7. The behaviour changes substantially from one model to another: it is apparent that the frequency content is different.

The frequency spectrum of the signal associated to the angular speed is depicted in Figs. 8 and 9, for $t > 50s$, after the transient effects vanish. The results from model M1 contain a main frequency that matches the fundamental one (0.45Hz). This is different for model M2, where the main frequency is close to the sixth natural frequency (7.40Hz), and the amplitudes associated to frequencies close to 0.45Hz are negligible, which explains the appreciable difference observed with the signals in the time-domain.

With regards to the run-time of the simulations, the calculations with M1 took 1 h 49 min, while for M2 3 h 56 min, showing an increase of 45%, recalling that 64 elements have been used for the torsional wave equation.

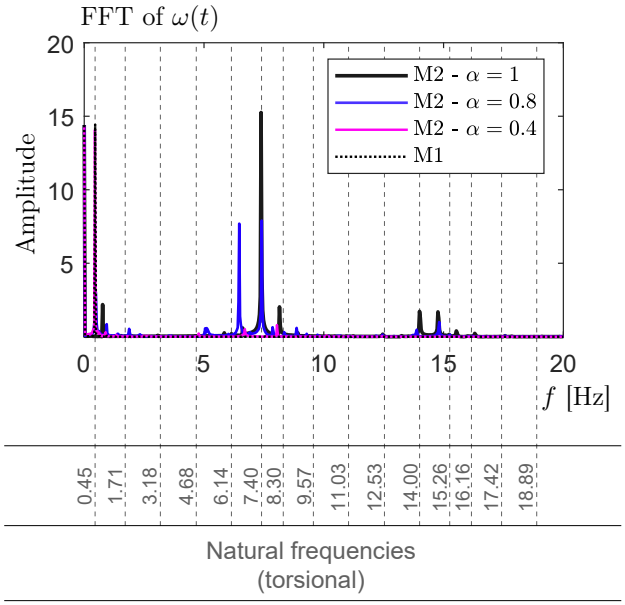


Figure 8: Simulation V2. FFT of the angular speed at the bit $\omega(t)$. Frequency range: 0 to 20Hz.

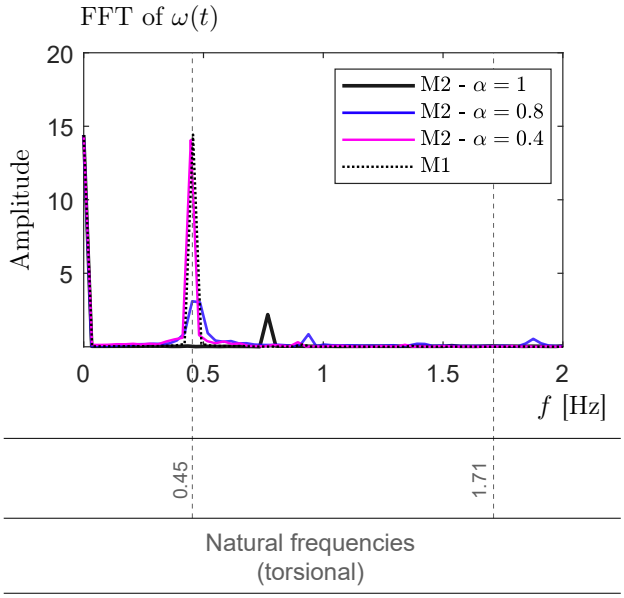


Figure 9: Simulation V2. Zoom of the FFT of the angular speed at the bit $\omega(t)$. Frequency range 0 to 2Hz.

## CONCLUSIONS

The modelling of the dynamics of a drill-string is not a simple task. Due to the variety of publications using different approaches to tackle their dynamics, the choice of an appropriate formulation not obvious, especially when long columns are simulated. For this reason, one of the motivations of this work is to discuss some of the the benefits and drawbacks of using either a low-dimensional lumped model or a continuous one. To do this, the predictions of an established 2-DOF approach (1-axial, 1-torsional) were compared with those of another model that considers a continuous torsional formulation plus 1-DOF for the axial dynamics. These models were named M1 and M2, respectively.

Without additional information, a continuous shaft model seems like the obvious choice for a slender and long structure like a drill-string, while a 1-torsional DOF representation is not. Low dimensional models are, by design, restricted in the amount of information that can be captured due to the number of DOF that are chosen beforehand. This is not an issue for a continuous approach. Only when the continuous formulation is solved numerically, there is a need to discretise the system of equations, leading to a finite number of DOF. But unlike lumped models, the selection is not arbitrary in continuous ones. It is made after a convergence analysis is carried out. This aspect is an advantage of continuous models that eliminates a potential source of discrepancy between the model's predictions and the real dynamics of the structure, by defining a minimum number of DOF that guarantees a certain level of accuracy. In addition, accurate and validated low-dimensional discrete models and continuous ones should provide similar results too, when the number of DOF in the discrete model is chosen correctly.

For this reason, to determine the usability and advantages of each formulation, first, a strategy to verify the newer model by including M1 as a particular case of model M2 was devised. For this task, an extra parameter, $\alpha$, was introduced. Through this parameter, the problem can be modified so that, for $\alpha \to 0$, the following assumptions hold: the drill-pipes are modelled in quasi-static conditions and the inertia becomes fully concentrated at the end of the string, instead of being distributed. The predictions obtained for small values of this parameter ($\alpha \to 0$) showed matching results with those already published in (Richard *et al.*, 2007), verifying some of the results given by model M2.

Second, a particular scenario was simulated with both models, taking $\alpha = 1$. The results were not similar, as the

responses did not match neither in the time domain nor the frequency domain.

The model M2, with the continuous approach, predicted an angular speed where, in comparison with the results with M1, higher frequencies are present. Then, although M1 is mathematically a correct derivation from M2, the discrepancy in the results shows that the quasi-static assumption clearly affects the accuracy of the simulations. In other words, the discrete model M1, which provides the same predictions as the model of (Richard *et al.*, 2007), is not an accurate representation of the continuous one. For this reason, the higher frequencies found with M2, the continuous torsional model, provide a hint in the direction of assuring that the 2-DOF could be an oversimplification of the problem, and that the approach may be inadequate to capture the dynamics of a real-scale drill-string.

Finally, the torsional formulation that has been used is conservative, with the exception of the forces and torques acting at the bit. In the simulations, the effects of the drilling fluids throughout the length of the structure were neglected, as well as the distributed contact. The authors expect that some damping might be introduced if these phenomena are taken into account, and that they could play some role in reducing the high frequencies that appear in model M2. Therefore, it is left for further work to asses the effect of other sources of damping that are not associated to the bit-rock interaction, such as internal structural damping and the effect of the drilling muds. Also, it is left for future work to explore the difference between these models, M1 and M2, and a continuous approach in both the axial and torsional formulations.

## ACKNOWLEDGEMENTS

This study was financed in part by the Brazilian institutions CAPES, FAPERJ and PUC-Rio, and by the Argentine institution CONICET.

## REFERENCES

Aarsnes, U.J.F. and van de Wouw, N., 2019. "Axial and torsional self-excited vibrations of a distributed drill-string". *Journal of Sound and Vibration*, Vol. 444, pp. 127–151. ISSN 10958568. doi:10.1016/j.jsv.2018.12.028. Publisher: Elsevier Ltd.

COMSOL AB, 2018. "COMSOL Multiphysics® v. 5.4".

Goicoechea, H.E., Buezas, F.S. and Rosales, M.B., 2019. "A non-linear Cosserat rod model for drill-string dynamics in arbitrary borehole geometries with contact and friction". *International Journal of Mechanical Sciences*, Vol. 157-158, No. March, pp. 98–110. ISSN 00207403. doi:10.1016/j.ijmecsci.2019.04.023. Publisher: Elsevier Ltd.

Goicoechea, H.E., Lima, R., Buezas, F. and Sampaio, R., 2022. "Drill-string with cutting dynamics: a mathematical assessment of two models". *To be published by Journal of Sound and Vibration*.

Lima, R. and Sampaio, R., 2015. "Stick-mode duration of a dry-friction oscillator with an uncertain model". *Journal of Sound and Vibration*, Vol. 353, pp. 259–271. ISSN 10958568. doi:10.1016/j.jsv.2015.05.015. Publisher: Elsevier.

Piovan, M.T. and Sampaio, R., 2009. "Modelos continuos de sondas de perforación para la industria petrolera: Análisis de enfoques y su discretización [continuum drill-string models for the oil industry: analysis of different approaches and their discretization]". *Revista Internacional de Metodos Numericos para Calculo y Diseno en Ingenieria*, Vol. 25, No. 3, pp. 259–277. ISSN 02131315.

Richard, T., Germay, C. and Detournay, E., 2007. "A simplified model to explore the root cause of stick-slip vibrations in drilling systems with drag bits". *Journal of Sound and Vibration*, Vol. 305, No. 3, pp. 432–456. ISSN 10958568. doi:10.1016/j.jsv.2007.04.015. ISBN: 0022460X.

Saldivar, B., Mondié, S., Niculescu, S.I., Mounier, H. and Boussaada, I., 2016. "A control oriented guided tour in oilwell drilling vibration modeling". *Annual Reviews in Control*, Vol. 42, pp. 100–113. ISSN 13675788. doi:10.1016/j.arcontrol.2016.09.002. Publisher: Elsevier Ltd.

Sampaio, R., Piovan, M.T. and Venero Lozano, G., 2007. "Coupled axial/torsional vibrations of drill-strings by means of non-linear model". *Mechanics Research Communications*, Vol. 34, No. 5-6, pp. 497–502. ISSN 00936413. doi:10.1016/j.mechrescom.2007.03.005. ISBN: 978-1-4020-4994-1.

Trindade, M.A. and Sampaio, R., 2005. "Modeling of Axial-Torsional Coupled Vibrations of Drill-Strings Drill-string Dynamics Modelling". *13th International Workshop on Dynamics and Control*.

Wahi, P. and Chatterjee, A., 2008. "Self-interrupted regenerative metal cutting in turning". *International Journal of Non-Linear Mechanics*, Vol. 43, No. 2, pp. 111–123. ISSN 00207462. doi:10.1016/j.ijnonlinmec.2007.10.010.

## RESPONSIBILITY NOTICE

The authors are the only responsible for the printed material included in this paper.